Performance analysis of a time-division-multiplexed fiber-optic gas-sensor array by wavelength modulation of a distributed-feedback laser

Wei Jin

The results of an investigation of the performance of a time-division-addressed fiber-optic gas-sensor array by means of wavelength modulation of a distributed-feedback (DFB) laser are reported. The system performance is found to be severely limited by the extinction ratio of the optical switch used for pulse amplitude modulation. Formulas that relate the cross-talk level to the extinction ratio of the switch, the modulation parameters of the DFB laser, and the optical path differences among sensing channels are derived. Computer simulation shows that an array of 20 methane gas sensors with a detection sensitivity of 2000 parts in 10^6 (ppm) (10-cm gas cell) for each sensor may be realized with a commercially available single Mach–Zehnder amplitude modulator (−35-dB extinction ratio). An array of 100 sensors with a 100-ppm detection sensitivity for each sensor may be realized if a double Mach–Zehnder amplitude modulator is used.

OCIS codes: 060.2370, 060.4230, 300.6260, 060.2310.

1. Introduction

Optical fiber gas sensors based on the absorption of light at near-IR wavelengths (1–1.8 μm) have attracted considerable attention over the past ten years or so.[1–9] The advantages of fiber sensors include their remote detection capability, safety in hazardous environments, and immunity to electromagnetic fields. The gases that can possibly be detected include methane, acetylene, hydrogen sulfide, carbon dioxide, and carbon monoxide.[1] Early optical gas sensors used light-emitting diodes (LED's) as light sources[2] and showed relatively low sensitivities. The broadband illumination bandwidth of the LED's means that other hydrocarbons also produce absorption. A Fabry–Perot comb filter tuned to the gas (methane) absorption-line spectrum demonstrated higher sensitivity and greatly enhanced selectivity within a fiber-coupled open-path bulk cell.[3]

Selectivity and sensitivity can be further enhanced by the use of distributed-feedback (DFB) lasers.[4–9] These sources give high spectral power densities within a linewidth that is narrower than a single absorption line in the absorption spectrum. Selectivity can be ensured by the laser's being tuned to a reference cell that contains the same gas as that to be monitored.[4,5,8] By wavelength modulation with a DFB laser and a synchronous detection technique, sensitivities down to less than 1 parts in 10^6 (with a 1-m-long equivalent gas cell) have been demonstrated.

The high sensitivity of the DFB system has allowed the use of simple short-path-length microcells but with preservation of a reasonable sensitivity that is adequate for many practical applications. The engineering of the sensor cells is greatly simplified, with a consequent reduction in cost, by use of the short path lengths that the high sensitivities allow. A sensitivity of better than 800 parts in 10^6 (ppm) has been demonstrated with a 25-cm micro-optic cell.[8] The sensitivity can be enhanced ten times by use of novel customized microcells and the proper wavelength modulation.[9,10] However, a single-cell system is of relatively high cost and has difficulty competing with catalytic-based sensors because of the high cost of the DFB lasers. A multiplexed array of low-cost micro-optic–cell sensors sharing the same DFB laser and the same signal processing unit would greatly reduced the cost in terms of cost per point. These

W. Jin is with the Department of Electrical Engineering, The Hong Kong Polytechnic University, Hung Hom, Kowloon, Hong Kong, China (e-mail, eejwei@poly.edu.hk).

Received 3 March 1999; revised manuscript received 14 May 1999.

0003-6935/99/255290-08$15.00/0

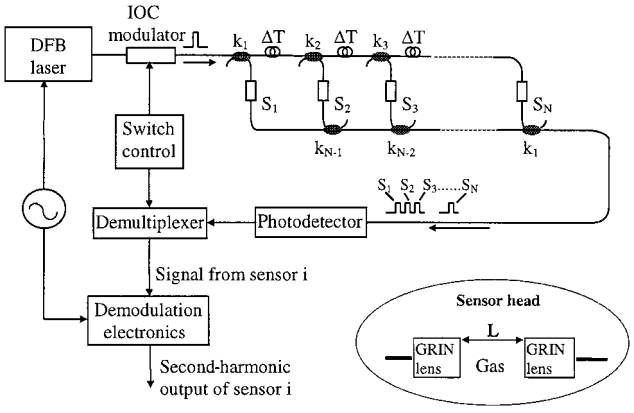

Fig. 1. Time-division-multiplexed ladder gas-sensor array. IOC, integrated optic circuit; GRIN, gradient index.

multipoint sensing systems would have a role to play in large-area gas-monitoring applications such as natural-gas–fired power plants,[11] coal mines, etc. In this paper I consider a time-division-multiplexed gas-sensor network of ladder array topology; I study the sensitivity limit of the sensor array and focus on the effect of a limited extinction ratio of the optical switch on the detection sensitivity of the sensors. An analysis of the performance as limited by shot noise is presented in Section 2; cross talk caused by incoherent and coherent effects due to the limited extinction ratio of the optical switch is discussed in Section 3; the performance of a particular methane gas-sensor array is presented in Section 4; a discussion of the effects of polarization, source coherence, and phase noise is given in Section 5; and a summary is presented in Section 6.

2. Shot-Noise–Limited Sensor Performance

Figure 1 shows the multiplexed gas-sensor system that we are going to analyze in the following sections. The system uses time-division addressing and a forward-coupled array topology. This topology was chosen because it can be efficiently used for multiplexing transmission-type gas sensors. Transmission-type gas sensors are preferred, as they have better performance than reflective-type sensors in minimizing the multipath interferometric effect and therefore provide better sensitivity.[9] The forward-coupled array topology is preferred to the normal ladder array configuration, as the forward-coupled array is more tolerant of the coupling ratios of the couplers required for balancing the sensor performance.[12]

It is assumed that the optical path differences between adjacent channels are the same. ΔT is the time-delay difference between adjacent sensors, and N is the number of sensor channels. If the period (τ) and the width (T_p) of the input optical pulse amplitude modulation satisfy the conditions

$$\Delta T \geq T_p, \qquad \tau \geq N\Delta T, \tag{1}$$

the pulses from different sensor channels will be separated in the time domain when they arrive at the photodetector and can be separated by electronic switching after photodetection. The optical power levels of different channels at the photodetector can be balanced if the coupling ratios of the couplers satisfy the condition[12]

$$k_j = \frac{1}{N-j+1}, \tag{2}$$

where k_j represents the coupling ratio of the jth coupler, as indicated in Fig. 1, for $j = 1, 2, \ldots N-1$. It is assumed that the peak power of the input pulses is P_0 and that the power losses associated with each individual sensor channel are the same and are equal to α_l^2. The peak power of each received pulse will be $\alpha_l^2 P_0/N^2$. The average optical power for each sensing channel and the total average optical power at the receiver will then be $(\alpha_l^2 P_0/N^2)(T_p/\tau)$ and $(\alpha_l^2 P_0/N)(T_p/\tau)$, respectively. The shot-noise current at the detector output is proportional to the square root of the total average optical power at the photodetector. Assuming that an ideal electric switch is used as the demultiplexer and that the switch is synchronized with the optical switch, the root-mean-square (rms) amplitude of the shot-noise current, after switching (demultiplexing), for each individual sensing channel may be expressed as[13]

$$i_{n,\mathrm{rms}} = \left(\frac{2qRB\alpha_l^2 P_0}{N^2}\frac{T_p}{\tau}\right)^{1/2}, \tag{3}$$

where R is the responsivity of the photodetector, q is the electron charge, and B is the detection bandwidth. For simplicity B is assumed to be the same for all sensor channels.

Consider a gas-sensing system that uses wavelength modulation, where the laser wavelength is locked to the center of the gas absorption through the use of a reference gas cell[4,5,8,9] and the second-harmonic signal is used as a measure of gas concentration; the rms value of the second-harmonic signal current for an individual sensor may be written as[14]

$$i_{2\omega,\mathrm{rms}} = \sqrt{2}Rk\alpha_0 CL\frac{\alpha_l^2 P_0}{N^2}\frac{T_p}{\tau}, \tag{4}$$

where C is the gas concentration, L is the interaction length (the length of the gas cell), and k is a dimensionless constant that depends on the amplitude of the wavelength modulation and the linewidth of the gas absorption line.[14] The gas absorption line is assumed to be collision broadened with a Lorentzian shape, and α_0 is the absorption coefficient for pure gas at the center of the absorption line.

The shot-noise–limited detection sensitivity for the second-harmonic detection technique can be obtained

with the second-harmonic signal, given by Eq. (4), set equal to the shot-noise contribution given by Eq. (3) and can be expressed as

$$\frac{\alpha_0 CL}{\sqrt{B}} = \frac{N}{k}\left(\frac{q}{R}\frac{1}{\alpha_l{}^2 P_0}\frac{\tau}{T_p}\right)^{1/2}. \tag{5}$$

The optimal result is obtained when $\Delta T = T_p$ and $NT_p = N\Delta T = \tau$, and the shot-noise–limited detection sensitivity can then be written as

$$\frac{\alpha_0 CL}{\sqrt{B}} = \frac{1}{k}\left(\frac{q}{R}\frac{N^3}{\alpha_l{}^2 P_0}\right)^{1/2}. \tag{6}$$

lation frequencies (e.g., less than 100 MHz), the laser output electric field may be expressed as[16]

$$E(t) = [P_0(1 + \eta \sin \omega t)]^{1/2} \times \exp\left[j2\pi\left(\nu_{L0}t + \nu_{Lm}\int_0^t \sin \omega u\,du\right)\right], \tag{7}$$

where ν_{L0} is the average laser frequency, ν_{Lm} is the amplitude of the frequency (wavelength) modulation, and η is the amplitude-modulation index.

Assuming a square pulse amplitude modulation with an extinction ratio[17] of $\alpha_e{}^2$, the electric field after the optical switch may be expressed as

$$E(t) = [P_0(1 + \eta \sin \omega t)]^{1/2} \exp\left[j2\pi\left(\nu_{L0}t + \nu_{Lm}\int_0^t \sin \omega u\,du\right)\right] \times \begin{Bmatrix} 1 & \text{for } m\tau \le t \le m\tau + T_p, \textit{ switch on} \\ \alpha_e \exp(j\phi) & \text{for } m\tau + T_p \le t \le (m+1)\tau, \textit{ switch off} \end{Bmatrix}, \tag{8}$$

3. Cross-Talk Analysis

In practice, other noises may well exceed the shot-noise level and limit the system performance. A major limiting factor for the system shown in Fig. 1 is the cross talk among different sensors caused by the nonideal optical switch used for input pulse generation. A practical optical switch has a limited extinction ratio; that is, when the switch is in an off state, there is still a small amount of light passing through the optical switch. The extinction ratio, which is defined as the ratio of the low power level (P_L, when the switch is off) and the high power level (P_H, when the switch is on), i.e., $\alpha_e{}^2 = 10 \log P_L/P_H$, is of the order of -30 to -35 dB for a single Mach–Zehnder switch and can reach -60 dB for a cascaded switch consisting of two Mach–Zehnder interferometers.[15] In this section we analyze the effect of this limited extinction ratio on the performance of the multiplexed system.

For a DFB laser with its wavelength modulated by current modulation, $i = i_0 + i_m \sin \omega t$ at low modulation frequencies (e.g., less than 100 MHz), the laser output electric field may be expressed as[16]

$$E(t) = [P_0(1 + \eta \sin \omega t)]^{1/2} \times \exp\left[j2\pi\left(\nu_{L0}t + \nu_{Lm}\int_0^t \sin \omega u\,du\right)\right], \tag{7}$$

where ν_{L0} is the average laser frequency, ν_{Lm} is the amplitude of the frequency (wavelength) modulation, and η is the amplitude-modulation index.

Assuming a square pulse amplitude modulation with an extinction ratio[17] of $\alpha_e{}^2$, the electric field after the optical switch may be expressed as

$$E(t) = [P_0(1 + \eta \sin \omega t)]^{1/2} \exp\left[j2\pi\left(\nu_{L0}t + \nu_{Lm}\int_0^t \sin \omega u\,du\right)\right] \times \begin{Bmatrix} 1 & \text{for } m\tau \le t \le m\tau + T_p, \textit{ switch on} \\ \alpha_e \exp(j\phi) & \text{for } m\tau + T_p \le t \le (m+1)\tau, \textit{ switch off} \end{Bmatrix}, \tag{8}$$

where $m = 0, 1, 2, \ldots$ and ϕ is a phase difference between the on and the off states that is caused by the optical switching.[18] The insertion loss of the switch has been omitted in the analysis, as it can be regarded as a reduction in the input power P_0.

The output electric field from the sensor array will be a summation of electric fields from all the individual sensors, i.e.,

$$E_0(t) = \sum_{i=1}^{N} E_{i0}(t), \tag{9}$$

with $E_{i0}(t)$ given by

$$E_{i0}(t) = \frac{\alpha_l}{N}\{P_0[1 + \eta \sin \omega(t - i\Delta T)]\}^{1/2} \exp\{-\alpha[\nu_{L0} + \nu_{Lm} \sin \omega(t - i\Delta T)]C_i L\} \times \exp\left\{j2\pi\left[\nu_{L0}(t - i\Delta T) + \nu_{Lm}\int_0^{t - i\Delta T} \sin \omega u\,du\right]\right\} \exp[j\varphi_i(t)] \times \begin{Bmatrix} 1 & \text{for } m\tau + i\Delta T \le t \le m\tau + i\Delta T + T_p \\ \alpha_e \exp(j\phi) & \text{for } m\tau + i\Delta T + T_p \le t \le (m+l)\tau + i\Delta T \end{Bmatrix}, \tag{10}$$

where $\alpha(\nu)$ is the amplitude absorption coefficient of the gas and $\varphi_i(t)$ is a random time-varying phasor that is due to the changing environment. Under atmospheric pressure the gas absorption line is collision broadened, and the line shape is given by a Lorentzian distribution.[14] The gas absorption also induces refractive-index changes and therefore phase changes of the light wave when it passes through the

gas cell. However, under the condition of low gas concentration such that $\alpha(\nu)CL \ll 1$, the phase variation caused by gas absorption can be neglected.[14]

In what follows we shall look at the demultiplexer output corresponding to channel i and study the performance limitation of channel i (sensor i) caused by cross talk from other sensors. To simplify the analysis, I use the following approximations:

$$\eta \sin \omega(t - i\Delta T) \approx \eta \sin \omega t,$$
$$\alpha[\nu_{L0} + \nu_{Lm} \sin \omega(t - i\Delta T)] \approx \alpha(\nu_{L0} + \nu_{Lm} \sin \omega t). \tag{11}$$

These approximations are useful in simplifying the analysis of the intensity-modulation– and the gas-absorption–related effects [the second and the third terms in the braces in Eq. (20)] and are correct for $i\omega\Delta T \ll \pi/2$, $i = 1, 2 \ldots, N - 1$. The use of these approximations will set an upper limit on the delay time (or maximum optical path length difference) between individual sensors. As the modulation frequencies used in practical modulation spectroscopy fiber gas sensors[4,5,8,9] are usually low ($\omega/2\pi < 30$ kHz), the optical path length difference allowed for satisfying this condition ($i\omega\Delta T \ll \pi/2$) can be reasonably long. Assuming $N\omega\Delta T \leq \pi/10$ (18°) for $f = 10$ kHz, we have $N\Delta T = 1/(20f) \leq 5$ μs, corresponding to a fiber length of 1 km. This length may already be longer than the coherence length of many DFB lasers.

The light intensity output from the sensor array can be calculated from Eqs. (9) and (10) and may be divided into four categories: the signal light intensity of channel i, $I_{0i}(t) = \langle|E_{i0}(t)|^2\rangle$; the light intensities from other channels (incoherent cross-talk terms), $I_{\text{inc}}(t) = \Sigma\langle|E_{j0}(t)|^2\rangle$, $j = 1, 2, \ldots, N$, $j \neq i$; mixing between the electric field of channel i and the other channels, $2\Sigma\ \text{Re}\langle E_{i0}(t)E_{j0}(t)\rangle$, $j = 1, 2, \ldots, N$, $j \neq i$, (here we call it the first-order coherent cross talk), where Re represents the real part; and mixing among the electric fields from channels other than channel i, i.e., $2\Sigma\ \text{Re}\langle E_{k0}(t)E_{m0}(t)\rangle$, $m = 1, 2, \ldots, N$, $k > m, k \neq i, m \neq i$ (second-order coherent cross talk).

Assuming that an ideal electric switch is used and synchronized with the input optical switch, the demultiplexed output that is used as the output for sensor i will pass the light signals only within the time interval $m\tau + i\Delta T < t < m\tau + i\Delta T + T_p$ ($m = 0, 1, 2 \ldots, i = 1, 2, \ldots, N$). The light signal within this time slot includes the four categories mentioned above. The signal intensity of channel i within this time interval may be expressed as

$$\begin{aligned} I_{i0}(t) &= \langle|E_{i0}(t)|^2\rangle \\ &= \frac{\alpha_l^2}{N^2} P_0(1 + \eta \sin \omega t) \\ &\quad \times \exp[-2\alpha(\nu_{L0} + \nu_{Lm} \sin \omega t)C_i L]. \end{aligned} \tag{12}$$

The incoherent cross talk may be expressed as

$$\begin{aligned} I_{\text{inc}}(t) &= \sum_{j=l,j\neq i}^{N} \langle|E_{j0}(t)|^2\rangle \\ &\approx \alpha_e^2 \frac{\alpha_l^2}{N^2} P_0(1 + \eta \sin \omega t) \\ &\quad \times \sum_{j=l,j\neq i}^{N} \exp[-2\alpha(\nu_{L0} + \nu_{Lm} \sin \omega t)C_j L]. \end{aligned} \tag{13}$$

The first-order coherent cross talk may be expressed as

$$\begin{aligned} I_{\text{co},1}(t) &\approx 2\alpha_e \frac{\alpha_l^2}{N^2} P_0(1 + \eta \sin \omega t) \sum_{j=1,j\neq i}^{N} \exp[-\alpha(\nu_{L0} \\ &\quad + \nu_{Lm} \sin \omega t)(C_i + C_j)L] \\ &\quad \times \cos\left[2\pi\nu_{L0}(i - j)\Delta T + \phi \right. \\ &\quad \left. + 2\pi\nu_{Lm} \int_{t-i\Delta T}^{t-j\Delta T} \sin \omega u\, du\right] \\ &\approx 2\alpha_e \frac{\alpha_l^2}{N^2} P_0(1 + \eta \sin \omega t) \sum_{j=1,j\neq i}^{N} \exp[-\alpha(\nu_{L0} \\ &\quad + \nu_{Lm} \sin \omega t)(C_i + C_j)L] \\ &\quad \times \cos(\phi_{i,j} + \phi + \zeta_{i,j} \sin \omega t), \end{aligned} \tag{14}$$

where

$$\zeta_{i,j} = \frac{4\pi\nu_{Lm}}{\omega} \sin \frac{\omega(i - j)\Delta T}{2}, \tag{15}$$

$$\phi_{i,j} = 2\pi\nu_{L0}(i - j)\Delta T + \varphi_i(t) - \varphi_j(t). \tag{16}$$

The second-order coherent cross talk may be expressed as

$$\begin{aligned} I_{\text{co},2}(\pm) &\approx 2\alpha_e^2 \frac{\alpha_l^2}{N^2} P_0(1 + \eta \sin \omega t) \sum_{m=1,m\neq i}^{N} \sum_{k>m,k\neq i}^{N} \\ &\quad \times \exp[-\alpha(\nu_{L0} + \nu_{Lm} \sin \omega t)(C_m + C_k)L] \\ &\quad \times \cos\left[2\pi\nu_{L0}(m - k)\Delta T + \varphi_m(t) - \varphi_k(t) \right. \\ &\quad \left. + 2\pi\nu_{Lm} \int_{t-m\Delta T}^{t-k\Delta T} \sin \omega u\, du\right] \\ &\approx 2\alpha_e^2 \frac{\alpha_l^2}{N^2} P_0 \sum_{m=1,m\neq i}^{N} \sum_{k>m,k\neq i}^{N} \cos(\phi_{m,k} \\ &\quad + \zeta_{m,k} \sin \omega t). \end{aligned} \tag{17}$$

In relation (17) we have neglected the effect of intensity modulation and the effect of gas absorption, as they are small compared with the direct interferometric effect.[9,14]

With the second harmonic taken as the output signal, for low gas concentration such that $\alpha_0 CL \ll 1$,

the average signal intensity can be obtained from Eq. (12) and is expressed as[14]

$$I_{2\omega} = 2k\alpha_0 CL \frac{\alpha_l^2 P_0}{N^2}. \tag{18}$$

Obviously, $I_{2\omega}$ is proportional to the second-harmonic signal current as given by Eq. (4) (with $T_p/\tau = 1$).

The second-harmonic amplitude of the incoherent cross talk can be obtained from relation (13) and is expressed as

$$I_{2\omega,\mathrm{inc}} = 2k\alpha_0\left(\sum_{j=1,j\neq i}^{N} C_j\right)L\alpha_e^2 \frac{\alpha_l^2}{N^2} P_0. \tag{19}$$

The second harmonic of the first-order coherent mixing term can be derived from relation (14) and is expressed as

$$\begin{aligned} I_{2\omega,\mathrm{co},1} = 2\alpha_e \frac{\alpha_l^2}{N^2} P_0 \sum_{j=1,j\neq i}^{N} \{&2\cos(\phi_{i,j} + \phi) J_2(\zeta_{i,j}) \sin 2\omega t \\ &+ \eta \sin(\phi_{i,j} + \phi)[J_1(\zeta_{i,j}) - J_3(\zeta_{i,j})]\cos 2\omega t \\ &- 2k\alpha_0(C_i + C_j)L[J_0(\zeta_{i,j}) - J_4(\zeta_{i,j})]\cos(\phi_{i,j} \\ &+ \phi)\sin 2\omega t\}, \end{aligned} \tag{20}$$

where $J_0, J_1, \ldots J_4$ are Bessel functions of the first kind. The three terms in the braces in Eq. (20) may be regarded as having different origins. The first term is directly caused by the interferometric effect, the second term is proportional to the intensity modulation, and the third term is proportional to gas concentrations. As we are interested in low gas concentrations, i.e., $\alpha_0 C_i L \ll 1$ ($i = 1, 2, \ldots, N$), and the value of η is usually small,[14] the first term is usually much larger than the other two terms.

The second harmonic of the second-order coherent cross talk may be obtained from relation (17) and is written as

$$\begin{aligned} I_{2\omega,\mathrm{co},2} = &4\alpha_e^2 \frac{\alpha_l^2}{N^2} \\ &\times P_0\left[\sum_{m=1,m\neq i}^{N} \sum_{k>m,k\neq i}^{N} \cos\phi_{m,k} J_2(\zeta_{\mathrm{m,k}})\right]\cos 2\omega t. \end{aligned} \tag{21}$$

By setting the signal given by Eq. (18) equal to that given by Eq. (19), we obtain the detection sensitivity in terms of minimum detectable gas concentration limited by incoherent cross talk (signal-to-noise ratio of 1) as

$$[C_i]_{\min} = \alpha_e^2 \sum_{j=1,j\neq i} C_j \leq \alpha_e^2 (N-1) C_{\max}, \tag{22}$$

where $C_{\max}$ represents the upper limit of gas concentration; for simplicity, we assume that it is the same for all the sensors.

By setting the signal given by Eq. (18) to the noise amplitude given by the first term in braces in Eq. (20), we can calculate the detection sensitivity determined by the first-order direct interferometric effect:

$$[\alpha_0 C_i L]_{\min} = \frac{2\alpha_e}{k} \sum_{j=1,j\neq i}^{N} J_2(\zeta_{i,j})\cos(\phi_{i,j} + \phi). \tag{23}$$

As ϕ_{ij} includes a random time-varying phasor $\varphi_i(t) - \varphi_j(t)$, it is logical to take the rms value of $[\alpha_0 C_i L]_{\min}$, i.e.,

$$[\alpha_0 C_i L]_{\min,\mathrm{rms}} = \frac{\sqrt{2}\alpha_e}{k}\left[\sum_{j=1,j\neq i}^{N} J_2^2(\zeta_{i,j})\right]^{1/2}. \tag{24}$$

The detection sensitivity limited by the amplitude-modulation factor can be obtained in a similar way by use of Eq. (18) and the second term in braces in Eq. (20) and is expressed as

$$[\alpha_0 C_i L]_{\min,\mathrm{rms}} = \frac{\sqrt{2}\alpha_e \eta}{2k}\left\{\sum_{j=1,j\neq i}^{N} [J_1(\zeta_{i,j}) - J_3(\zeta_{i,j})^2]\right\}^{1/2}. \tag{25}$$

The detection sensitivity set by the gas-concentration–related cross talk can be obtained by use of Eq. (18) and the third term in braces in Eq. (20) and is expressed as

$$\begin{aligned} [C_i]_{\min} = &2\alpha_e \sum_{j=1,j\neq i}^{N} [J_0(\zeta_{i,j}) - J_4(\zeta_{i,j})] \\ &\times \cos(\phi_{i,j} + \phi)(C_i + C_j). \end{aligned} \tag{26}$$

Under the condition that $C_i \to 0$, the rms value of $[C_i]_{\min}$ may be expressed as

$$\begin{aligned} [C_i]_{\min,\mathrm{rms}} &= 2\alpha_e\left\{\sum_{j=1,j\neq i}^{N} [J_0(\zeta_{i,j}) - J_4(\zeta_{i,j})]^2 (C_j^2)\frac{1}{2}\right\}^{1/2} \\ &\leq \sqrt{2}\alpha_e C_{\max}\left\{\sum_{j=1,j\neq i}^{N} [J_0(\zeta_{i,j}) - J_4(\zeta_{i,j})]^2\right\}^{1/2}. \end{aligned} \tag{27}$$

The detection sensitivity limited by the second-order coherent cross talk can be obtained by use of Eqs. (18) and (21),

$$[\alpha_0 C_i L]_{\min,\mathrm{rms}} = \frac{\sqrt{2}\alpha_e^2}{k}\left[\sum_{m=1,m\neq i}^{N} \sum_{k>m,k\neq i}^{N} J_2^2(\zeta_{m,k})\right]^{1/2}. \tag{28}$$

There are $(N^2 - 3N + 2)/2$ terms in the summation in the square root. Comparing the second-order with the first-order coherent cross talk, the second-order effect is proportional to α_e^2 instead of α_e; however, there are $(N^2 - 3N + 2)/2$ terms for the second-order effects instead of N terms as for the first-order effect.

Relations (6), (22), (24), (25), (27), and (28) can be used to evaluate the sensitivities of sensors limited by shot noise and by various interferometric-related effects.

4. Performance of a Methane Gas-Sensor Array

Here we consider a particular methane gas-sensor array that is based on absorption at 1665.5 nm [$Q(6)$ line, Ref. 14]. At this wavelength the absorption coefficient is $\alpha_0 \approx 0.1\ \mathrm{cm}^{-1}$. The length of the gas cell is assumed to be $L = 10$ cm, giving $\alpha_0 L \approx 1$. The amplitude of the frequency modulation is approximately twice the linewidth of the $Q(6)$ line and is ~4 GHz. This gives a scale factor of $k \approx 0.34$, corresponding to the theoretical optimal value for the second-harmonic detection technique.[14] Other system parameters[14] are $P_0 = 2$ mW, $\alpha_l^2 = 0.6$, $\eta = 0.2$, $q = 1.6 \times 10^{-19}$ C, $R = 0.55$. Here I report the performance of sensor 1, which I evaluate by using relations (6), (22), (24), (25), (27), and (28) and setting $i = 1$. The performances of other sensors were evaluated in the same way, with i set to different integers from 2 to N, and were found to be more or less the same as sensor 1.

The shot-noise–limited detection sensitivity as a function of sensor number can be obtained from Eq. (6) and is $[C]_s/(B)^{1/2} = 4.6 \times 10^{-8} N^{3/2}/\mathrm{Hz}^{1/2}$. For a sensor array of as many as 100 sensors, $[C]_s/(B)^{1/2}$ is below 50 ppm/$\mathrm{Hz}^{1/2}$.

The minimum detectable gas concentration limited by incoherent cross talk increases linearly with the sensor number and is proportional to the extinction ratio α_e^2 [Eq. (22)]. Assuming that the maximum measurable gas concentrations for all the sensors in the array are the same and are $C_{\max} = 5\%$, for a commercially available single Mach–Zhender amplitude modulator (switch) of extinction ratio −30 dB ($\alpha_e^2 = 10^{-3}$), to achieve 1000-ppm sensitivity, the maximum sensor number is 20. To realize a sensor array of 100 sensors and of the same sensitivity, the required extinction ratio set by incoherent cross talk is less than 37 dB. For a double Mach–Zhender amplitude modulator of extinction −60 dB, the detection sensitivity can be as small as 5 ppm.

Figure 2 shows the sensor performance limited by the direct interferometric effect as a function of the time-delay difference between adjacent channels [calculated from Eq. (24)] for various sensor numbers at a modulation frequency of 10 kHz. The upper curve in the figure is for $N = 100$, and the lower curve is for $N = 20$. The vertical axis is normalized by α_e, the square root of the extinction ratio of the switch. For a particular extinction ratio, e.g., −40 dB ($\alpha_e^2 = 10^{-4}$), one can obtain the minimum detectable gas concentration simply by multiplying the value shown on the vertical axis by $\alpha_e = 10^{-2}$. It can be seen from Fig. 2 that the sensor resolution can be improved by approximately 5 and 10 times when the delay between sensors is increased from close to zero to $\Delta T = 20$ ns and $\Delta T = 100$ ns, respectively. This corresponds to 4 and 20 m in terms of the difference in fiber lengths between the adjacent sensor channels. These results are expected because, for low modulation frequencies, the modulation index ζ_{ij} as defined in Eq. (15) can be approximated as $\zeta_{ij} \approx 2\pi\nu_{Lm}\omega(i - j)\Delta T$. An increase in ΔT will increase the value of ζ_{ij} and would in general result in a decrease in $J_2(\zeta_{ij})$. When the modulation frequency is high (e.g., 100 MHz), the above approximation will not hold and ζ_{ij} will vary periodically with ΔT because of the $\sin \omega(i - j)\Delta T$ dependence as implied by Eq. (15). The interferometric effect thus cannot be reduced by the delay's being increased between sensors. At 10 kHz, for $\alpha_e^2 = -35$ dB and $\alpha_e^2 = -60$ dB, the minimum detectable gas concentration (for $\Delta T = 100$ ns, $N = 20$ or $N = 100$) is ~2000 and ~100 ppm, respectively.

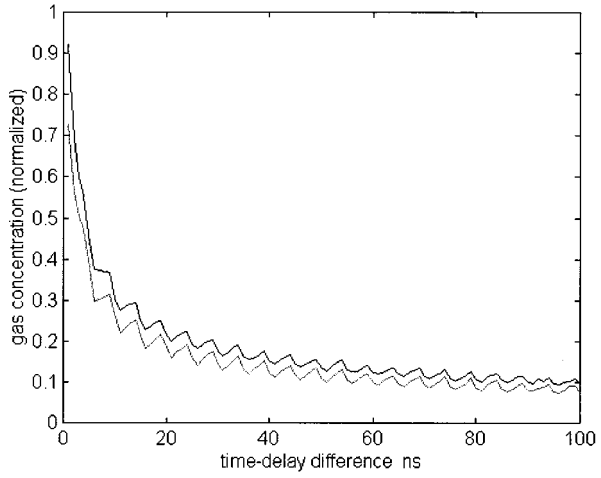

Fig. 2. Normalized minimum detectable gas concentration $\{[C_1]_{\min,\mathrm{rms}}/\alpha_e$, calculated from Eq. (24)$\}$ versus time-delay difference (ΔT) between sensor channels. $f = 10$ kHz; upper curve, $N = 100$; lower curve, $N = 20$.

Figure 3 shows the minimum detectable gas concentration determined by the amplitude-modulation–related effect at a modulation frequency of 10 kHz. The modulation characteristics are similar to those for a direct interferometric effect, except that the magnitude is approximately one fourth as large. We

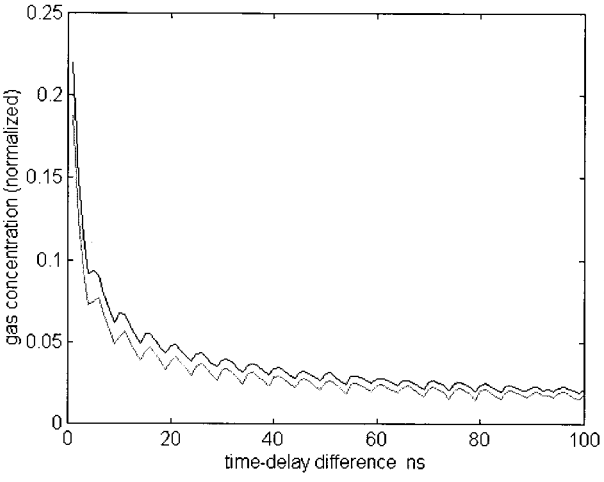

Fig. 3. Normalized minimum detectable gas concentration $\{[C_1]_{\min,\mathrm{rms}}/\alpha_e$, calculated from Eq. (25)$\}$ versus time-delay difference (ΔT) between sensor channels. $f = 10$ kHz; upper curve, $N = 100$; lower curve, $N = 20$.

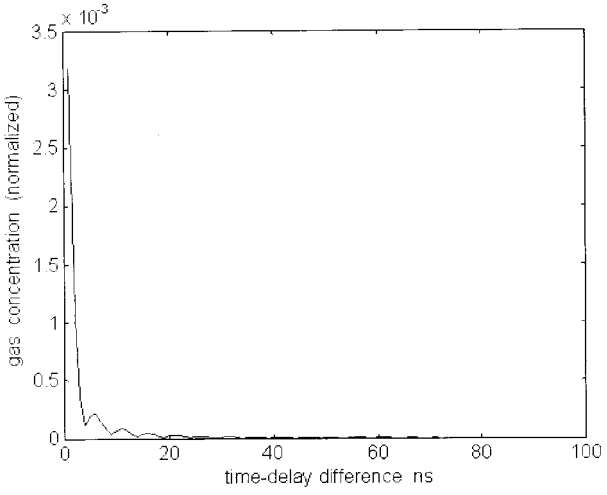

Fig. 4. Normalized minimum detectable gas concentration $\{[C_1]_{\min,\mathrm{rms}}/\alpha_e$, calculated from relation (27)$\}$ versus time-delay difference (ΔT) between sensor channels. $f = 10$ kHz; for $N = 20$ or $N = 100$, the results are the same.

may need to consider this effect once the direct interferometric effect is minimized.

Figure 4 shows the minimum detectable gas concentration determined by the gas-absorption–related effect at a modulation frequency of 10 kHz. This effect shows a similar trend as and is much smaller than the two effects mentioned above.

Figure 5 shows the minimum detectable gas concentration limited by the effect of second-order coherent cross talk as a function of time-delay differences between adjacent channels. In Fig. 5 the values shown on the vertical axes are normalized by $\alpha_e{}^2$ instead of α_e. At a low modulation frequency (10 kHz), for $\alpha_e{}^2 = -35$ dB and $\Delta T = 100$ ns, the minimum detectable gas concentration for $N = 20$ is ~500 ppm. It can increase to 4000 ppm for $N = 100$.

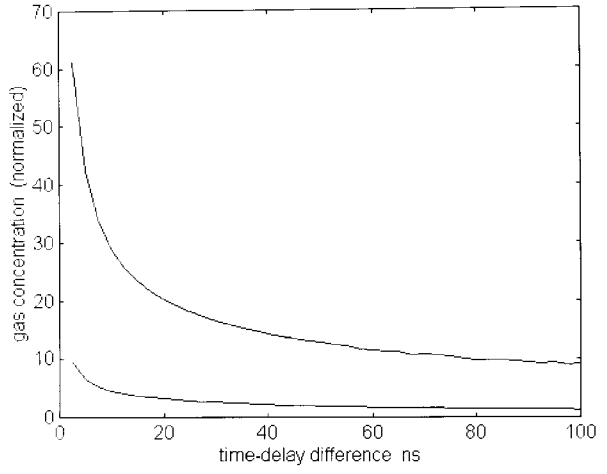

Fig. 5. Normalized minimum detectable gas concentration limited by the second-order interferometric effect $\{[C_1]_{\min,\mathrm{rms}}/(\alpha_e)^2$, calculated from Eq. (28)$\}$ versus time-delay difference (ΔT) between sensor channels. $f = 10$ kHz; upper curve, $N = 100$; lower curve, $N = 20$.

This value is higher than the first-order interferometric effect, implying that for a large array with a low-extinction-ratio optical switch, the second-order effect could be dominant. For $\alpha_e{}^2 = -60$ dB, the minimum detectable gas concentration limited by the second-order coherent cross talk for $N = 100$ is of the order of 10 ppm.

5. Discussion

In Section 3 we assumed that the polarization states of different sensor channels are the same. In practical systems with single-mode optical fibers, the polarization states in different channels may be different and may change randomly with environmental disturbances. The effect of the different polarization states is to reduce the magnitude of the mixing terms as given by relations (14) and (17), which in turn reduces the magnitude of the coherent cross talk. A factor of $\cos \theta_{i,j}$ $(i, j = 1, 2, \ldots, N, i \neq j)$ may be inserted into the right-hand side of relations (14) and (17) to account for the polarization effect. Here θ_{ij} represents an angle between the polarization vectors of channel i and channel j. If we assume that each θ_{ij} varies randomly and independently of the others, the rms value of the lower detection limit given by relations (24), (25), (27), and (28) should be multiplied by a factor of $1/\sqrt{2}$.

In the discussion in Section 3 we have also assumed that the source coherence length is very long, longer than the optical path difference between the first sensing channel and the last sensing channel ($L_c > N\Delta Tc/n$). In practice, however, the source coherence is limited, and for typical DBF lasers the source linewidth is of the order of 10–100 MHz, corresponding to a coherence length of 10–100 m. For the case of limited coherence lengths, the coherence-related cross talk may be analyzed in a way similar to the following: We again look at the performance of sensor 1. If the coherence time ($\tau_c = L_c/c$) of the source satisfies $l\Delta T < \tau_c < (l + 1)\Delta T$, only signals from channels 2, 3, . . . , l would contribute significantly to the first-order coherence-related cross talk. The lower detection limit of sensor 1 can be calculated from relations (24), (25), and (27) with $i = 1$ and with N replaced with l. As $l < N$, the cross talk should be reduced compared with the case of an infinitely long coherence length. Consider a particular case in which $\Delta T < \tau_c < 2\Delta T$: Only the second sensor will contribute significantly to the first-order coherence-related cross talk; contribution from other sensors should be negligible. For the second-order coherence-related cross talk, the situation becomes slightly complicated. However, the cross talk may be calculated by one's considering only those terms in Eq. (28) that satisfy the condition $|m - k|\Delta T < \tau_c$. When $\tau_c \ll \Delta T$, all first- and second-order interference terms should vanish, and the system performance would be limited only by the incoherent effect, which can be evaluated by use of Eq. (22).

Because the sensing system is characterized by many paths, the laser phase noise will be converted into intensity noise and limit the system perfor-

mance. The laser-phase-induced intensity noise in an interferometer system has been studied in detail by Moslesi,[19] and for our applications the ratio of laser-phase-induced intensity noise to the power of coherent cross talk that is due to the limited extinction ratio of the optical switch is found to be less than $B\tau_c$. Here τ_c is the coherence time of the DFB laser. Assuming a DFB laser with a 10-MHz linewidth and a detection bandwidth of 10 Hz, $B\tau_c$ should be less than 10^{-6}, indicating that the laser-phase-noise contribution is much less than the cross talk caused by coherent or incoherent effects arising from the limited extinction ratio of the optical switch.

6. Summary

The performance of a time-division-addressed gas-sensor array with a ladder topology has been examined. It has been found that the system performance depends strongly on the extinction ratio of the optical switch used. For an optical switch with an extinction ratio of −35 dB and a gas cell 10 cm long, a methane gas-sensor array of as many as 20 sensors with detection sensitivities of 2000 ppm for each sensor may be realized by use of low-frequency modulation and an appropriate delay between sensing channels (>100 ns or 20 m). With an optical switch with an extinction ratio of −60 dB, the minimum detectable gas concentration may be reduced to 100 ppm.

The author acknowledges helpful discussions with B. Culshaw and G. Stewart of Strathclyde University. This work is partly supported by the Hong Kong Research Grants Council under Competitive Earmarked Research Grant PolyU 5081/98E.

References

1. G. Stewart, "Fibre optic sensors," *Sensor Systems for Environmental Monitoring, Vol. 1: Sensor Technologies*, M. Campbell, ed. (Chapman & Hall, London, 1997), Chap. 1, pp. 1–40.
2. K. Chan, H. Ito, H. Inaba, and T. Furuya, "10 km-long fiber optic remote sensing of CH_4 gas by near infrared absorption," Appl. Phys. B, **38,** 11–15 (1985).
3. J. P. Dakin, C. A. Wade, D. Pinchbeck, and J. S. Wykes, "A novel optical fibre methane sensor," J. Opt. Sensors **2,** 261–267 (1987).
4. K. Uehara and H. Tai, "Remote detection of methane using a 1.66-μm diode laser," Appl. Opt. **31,** 809–814 (1992).
5. K. Yamamoto, H. Tai, M. Uchida, S. Osawa, and K. Uehara, "Long distance simultaneous detection of methane and acetylene by using diode lasers in combination with optical fibers," *Proceedings of Eighth Optical Fiber Sensors Conference*, (Institute of Electrical and Electronics Engineers, New York, 1992), pp. 333–336.
6. V. Weldon, P. Phelan, and J. Hegarty, "Methane and carbon dioxide sensing using a DFB laser diode operating at 1.64 μm," Electron. Lett. **29,** 560–561 (1993).
7. Y. Shimose, T. Okamoto, A. Maruyama, M. Aizawa, and H. Nagai, "Remote sensing of methane gas by differential absorption measurement using a wavelength-tunable DFB LD," IEEE Photon. Technol. Lett. **3,** 86–87 (1991).
8. W. R. Philp, W. Jin, A. Mencaglia, G. Stewart, and B. Culshaw, "Interferometric noise in frequency modulated optical gas sensors," in *Proceedings of Twenty-first Australian Conference on Optical Fibre Technology* (IREE Society, Milsons Point, Australia, 1986), pp. 185–188.
9. G. Stewart, A. Mencaglia, W. Philp and W. Jin, "Interferometric signals in fiber optic methane sensors with wavelength modulation of the DBF laser source," J. Lightwave Technol. **16,** 43–53 (1998).
10. M. A. Morante, G. Stewart, B. Culshaw, and J. M. Lpoezhiguera, "New micro-optic cell for optical-fiber gas sensor with interferometric noise-reduction," Electron. Lett. **33,** 1407–1409 (1997).
11. *Brochure of Black Point Combined Cycle Power Station Project* (China Light & Power Co., Ltd, Hong Kong, 1997).
12. A. D. Kersey, A. Dandridge, A. R. Davis, C. K. Kirdendall, M. J. Marrone, and D. G. Gross, "64-element time-division multiplexed interferometric sensor array with EDFA telemetry," in *Optical Fiber Communications Conference*, Vol. 2 of 1996 OSA Technical Digest Series (Optical Society of America, Washington, D.C., 1996), pp. 270–271.
13. J. L. Brooks, B. Moslehi, B. Y. Kim, and H. J. Shaw, "Time-domain addressing of remote fiber optic interferometric sensors arrays," J. Lightwave Technol. **LT-5,** 1014–1023 (1987).
14. W. Jin, Y. Z. Xu, M. S. Demokan, and G. Stewart, "Investigation of interferometric noise in fiber-optic gas sensors with use of wavelength modulation spectroscopy," Appl. Opt. **36,** 7239–7246 (1997).
15. C. K. Kirkendall, A. R. Davis, and A. Dandridge, "High extinction ratio optical switch and bias control," in *Optical Fiber Sensors*, Vol. 16 of 1997 OSA Technical Digest Series, (Optical Society of America, Washington, D.C., 1997), pp. 560–563.
16. A. Yariv, *Optical Electronics in Modern Communications*, 5th ed. (Oxford U. Press, New York, 1997), pp. 587–596.
17. S.-C. Huang, W.-W. Lin, and M.-H. Chen, "Cross-talk analysis of time-division multiplexing of polarization-insensitive fiber-optic Michelson interferometric sensors with a 3 × 3 directional coupler," Appl. Opt. **36, 4,** 921–933 (1997).
18. J. C. Cartledge, "Comparison of effective α-parameters for semiconductor Mach–Zehnder optical modulator," J. Lightwave Technol. **16,** 372–378 (1998).
19. B. Moslehi, "Noise power spectra of optical two-beam interferometers induced by laser phase noise," J. Lightwave Technol. **LT-4,** 1704–1710 (1986).